Published in final edited form as:
Ultrasound Med Biol. 2007 January ; 33(1): 48–56.

IMPROVEMENT OF ELASTOGRAPHIC DISPLACEMENT ESTIMATION USING A TWO-STEP CROSS-CORRELATION METHOD

Hao Chen[*,†], **Hairong Shi**[*], and **Tomy Varghese**[*]
* *Department of Medical Physics, The University of Wisconsin-Madison, Madison, Madison, WI, USA; and*

†*Department of Electrical and Computer Engineering, The University of Wisconsin-Madison, Madison, WI, USA*

Abstract

The cross-correlation algorithm used to compute the local strain components for elastographic imaging requires a minimum radio-frequency data segment length of around 10 wavelengths to obtain accurate and precise strain estimates with a reasonable signal-to-noise ratio. Shorter radio-frequency data segments generally introduce increased estimation errors as the information content in the data segment reduces. However, shorter data segments and increased overlaps are essential to improve the axial resolution in the strain image. In this paper, we propose a two-step cross-correlation technique that enables the use of window lengths on the order of a single wavelength to provide displacement and strain estimates with similar noise properties as those obtained with a 10 wavelength window. The first processing step utilizes a window length on the order of 10 wavelengths to obtain coarse displacement estimates between the pre- and postcompression radio frequency data frames. This coarse displacement is then interpolated and utilized as the initial guess-estimate for the second cross-correlation processing step using the smaller window. This step utilizes a single wavelength window to improve the axial resolution in strain estimation, without significantly compromising the noise properties of the image. Simulation and experimental results show that the signal-to-noise and contrast-to-noise ratio estimates improve significantly at the smaller window lengths with the two-step processing when compared with the use of a similar sized window in the currently utilized single window method.

Keywords

Cross-correlation; Elastography; Elasticity; Strain; Resolution; Signal-to-noise ratio; Contrast-to-noise ratio

INTRODUCTION

Elastography or techniques that image the local stiffness properties of tissue is a relatively new technique for noninvasive investigation of tissue mechanical properties (Ophir et al. 1991; Cespedes et al. 1993; O'Donnell et al. 1994; Talhami et al. 1994; Chen et al. 1995; Bilgen and Insana 1996; Zhu and Hall 2002). In elastography local strains are obtained by computing the gradient of the displacement field along the axial direction between the pre- and postcompression echo signal frames obtained after a quasistatic compression. Local strain

Address correspondence to: Tomy Varghese, Department of Medical Physics, The University of Wisconsin-Madison, Madison, WI 53706, USA. E-mail: tvarghese@wisc.edu.

images are interpreted based on the fact that stiffer tissues deform less than softer tissues under identical compressional forces, thereby providing a relative comparison of the stiffness variations in tissue.

The normalized cross-correlation algorithm for strain estimation (Ophir et al. 1991) is one of the most commonly used methods, where the shift in the peak of the cross-correlation function is utilized to track tissue deformation. However, for 1-D strain estimation, we require a window length of at least 10 wavelengths to obtain accurate and precise strain estimates, as also illustrated in this paper. This requirement on the window length precludes the use of smaller gated window lengths that would otherwise enable improvement in the axial resolution of the strain images. The use of smaller window lengths is important, since Righetti et al. (2002), have demonstrated that the ultimate axial resolution in elastography is only limited by and directly proportional to the wavelength (*i.e.*, inversely proportional to the fractional bandwidth) of the ultrasound system. To enable the use of smaller window lengths, we propose the use of a two-step cross-correlation method, where we demonstrate accurate and precise strain estimation with window lengths on the order of a single wavelength. The method proposed in this paper is not limited to 1-D techniques and are scalable to 2-D and 3-D strain estimation kernels.

Other approaches where multiple window lengths have been utilized to obtain strain images include multiresolution (Varghese et al. 1998) and multiscale (Pellot-Barakat et al. 2004) approaches. In the multiresolution approach (Varghese et al. 1998), a composite strain images was constructed by selecting local strains with the highest elastographic signal-to-noise ratio (SNR_e) estimated from several elastograms obtained using multiple window lengths. The multiscale technique (Pellot-Barakat et al. 2004), on the other hand, relies on the estimation of dense displacement fields by the coarse-to-fine minimization of an energy function that combines constraints of conservation of echo amplitude and displacement field continuity. A combination of envelope and radio-frequency (RF) signal processing have also been used (Cespedes 1993; Varghese and Ophir 1998; Yamakawa and Shiina 2001) to reduce the peak-hopping errors observed with the use of only RF signals. Envelope signals are first used to obtain a coarse estimate of the displacement, with a finer estimate of the displacement (in the neighborhood of the coarse displacement estimate) obtained using RF signals.

Other algorithms that have been utilized for strain estimation include adaptive stretching (Alam et al. 1998; Brusseau et al. 2000; Srinivasan et al. 2002), staggered strain estimation (Srinivasan et al. 2002), 2D block-matching (Chaturvedi et al. 1998; Hall et al. 2003) and 2D cross-correlation (Shi and Varghese 2006) techniques.

In the single window cross-correlation method, the selection of the window length is a trade-off between the attainable resolution and noise level within the strain image (Varghese et al. 1998), In this paper, we illustrate that the two-step cross-correlation technique provides high resolution strain images (obtained using window lengths on the order of a single wavelength) without sacrificing the SNR_e or contrast-to-noise (CNR_e) ratio in the elastogram. Simulation results show that the SNR_e and CNR_e estimates obtained using the smaller window lengths with the two-step processing are significantly higher when compared with the use of a similar-sized window in the currently utilized single window method. Experimental results also demonstrate the ability to obtain elastograms with a high SNR_e and CNR_e using an initial window of 10 wavelengths and the second window that corresponds to only a single wavelength.

MATERIALS

The two-step cross-correlation algorithm

In the traditional cross-correlation algorithm, similar-sized data segments at the same depth in tissue from the pre- and postcompression RF echo signal data are compared. However, due to the applied compression and resultant deformation of tissue scatterers, the echo-signal information regarding the scatterers contained within the gated precompression data segment may not lie within the gated postcompression data segment at the same depth. In other words, due to the deformation of the scatterers, the actual segment location would be shifted down in depth relative to the applied compression. In addition, this discrepancy in the signal information also increases with depth into tissue.

Several investigators have recognized this problem and have attempted to correct for the translation of the postcompression echo signal. One of the initially utilized techniques was to use a larger sized gated postcompression data segment, providing an opportunity for the smaller gated precompression data segment to find the best match (Cespedes et al. 1993). Another approach was to utilize global temporal stretching, where the postcompression echo signal was stretched by the average value of the compression, thereby reducing echo-signal mismatches (Cespedes et al. 1993; Varghese and Ophir 1996; Alam and Ophir 1997). Global stretching, however, introduces artifacts when regions of varying stiffness are present (inhomogeneous tissue), where some regions may be overstretched while other regions are understretched (Varghese et al. 2001). The trade-offs associated with many of these approaches are discussed by Varghese et al. (2001).

Most of the methods discussed above require the use of window lengths on the order of at least 10 wavelengths (as shown in this paper) to obtain accurate local strain estimation results. Methods that utilize 2-D kernels that are generally a fraction of the wavelength along the axial dimension (Zhu and Hall 2002; Pellot-Barakat et al. 2004) utilize error correction techniques and reduced search regions to reduce displacement estimation errors. They also operate under the assumption or constraint that the displacement field would be continuous and along the direction of compression (generally axial), with expansion only along the lateral and elevational directions. The use of smaller kernels for 2D processing indicate the possibility of using smaller window lengths, thereby improving the axial resolution (Alam et al. 2000; Righetti et al. 2002) for 1D cross-correlation, if these gated windows could be accurately localized within the postcompression echo signals.

The two-step cross-correlation method proposed in this paper attempts to overcome some of the limitations discussed above by estimating local displacements in two steps. In the first step, a larger window length (>10 wavelengths), with no overlapping of the data segments in the cross-correlation processing, is utilized to obtain a coarse but high signal-to-noise estimate of the local displacement. A second-order polynomial fit is then utilized to interpolate the local displacement estimates obtained in the first correlation step, to obtain finer local displacement estimates that are utilized as initial guess-estimate values, to refine the displacement estimation in the second correlation step. In the second cross-correlation processing step, the smaller single wavelength window is utilized to estimate the local displacement. The interpolated displacement map generated in the first correlation step guides the placement of the gated postcompression data segment within the postcompression echo signals. The postcorrelation data segment used in the second processing step, therefore, may no longer be at the exact same depth as the gated precompression data segment (depending on the tissue deformation), but offset by the displacement obtained from the first correlation step. Prior knowledge of the displacement pattern obtained during the initial or first processing step, therefore, enables the algorithm to compare the pre- and postcompression echo signals generated by the same set of tissue scatterers to obtain reliable, fine and high SNR displacement estimates using single

wavelength windows. The flow chart presented in Fig. 1 shows the operation of the two-step cross-correlation algorithm.

Axial resolution in elastography depends on two signal processing parameters, namely, the cross-correlation window length and the amount of overlap in the data segments between successive windows (Cespedes 1993; Bilgen and Insana 1997; Alam et al. 2000; Righetti et al. 2002). The cross-correlation window length at a fixed overlap was initially utilized as a measure of the axial resolution in elastography (Cespedes 1993). Alam et al. (2000) derived an empirical expression for the axial resolution as a bilinear function of the window length and overlap, with the overlap being more dominant. In general, longer-duration windows are preferred for improved sensitivity, dynamic range and SNR_e; however, the elastogram is degraded due to poor resolution. Increasing the window length leads to a loss of resolution in the strain image. Increasing the overlap, on the other hand, improves the resolution of the elastogram, with the disadvantage of reduced SNR_e due to increased noise contributions. However, the best noise performance is obtained with no overlapping of the data segments, which is, however, not practical for strain imaging. Trade-offs between the SNR_e and CNR_e improvement and axial resolution have also been previously discussed (Srinivasan et al. 2003; Srinivasan et al. 2004). As mentioned earlier in this paper, Righetti et al. (2002) have shown that the axial resolution in elastography is ultimately limited by the wavelength of the ultrasound system. In this paper, we demonstrate that strain estimation on the order of a single ultrasound wavelength can be achieved using the two-step algorithm.

Both simulations and tissue-mimicking (TM) phantom experiments are utilized to evaluate the performance of the two-step cross-correlation algorithm. The simulations are focused on evaluating improvements in the axial resolution obtained using this technique when compared with the traditional cross-correlation method. Experimental results on phantoms evaluate the SNR_e and CNR_e improvements obtained using uniformly-elastic and single-inclusion phantoms, respectively.

METHODS

Simulation

The simulated phantom was constructed using a commercial finite element analysis (FEA) package ANSYS (ANSYS Inc., Pittsburgh, PA, USA) and an ultrasound simulation program developed in our laboratory (Li and Zagzebski 1999). We constructed a numerical TM phantom with dimensions 40 × 40 × 10 mm with two embedded small cylindrical inclusions with a 2 mm diameter ten times stiffer than the background. The separation between the two cylindrical inclusions was varied in units of 1 mm to obtain inclusions separated by 1, 2, 3 and 4 mm, as shown in Fig. 2(a), respectively. The FEA program ANSYS was used to construct the phantom and to apply the uniform external deformation of 0.5% of the phantom height.

The pre- and postcompression ultrasound RF echo signals were obtained using a frequency-domain clinical ultrasound simulation program developed by Li and Zagzebski (1999). A linear array transducer was modeled, consisting of 0.1 × 10 mm elements with a 0.1 mm center-to-center separation. Each acoustic beam was formed using 64 consecutive elements. The incident pulses were modeled to be Gaussian-shaped with a 7.5 MHz center frequency and an 80% bandwidth (full-width at half-maximum). The speed of sound in the simulation was 1540 m/s and the attenuation coefficient was set to 0.5 dB/cm/MHz for both the inclusion and background. The scatterers were modeled using 100 μm radius polystyrene beads, which were randomly distributed in the numerical phantom at a sufficient number density to obtain Rayleigh statistics (Wagner et al. 1983). The postcompression signal was obtained by displacing the scatterer positions in accordance with the FEA displacements obtained due to the modeled mechanical stimuli described above. The simulated pre- and post-compression

echo signals obtained were then utilized to evaluate the two-step and the traditional cross-correlation algorithm.

Experiment

The single inclusion TM phantom with dimensions of 80 × 80 × 100 mm manufactured in our laboratory (Madsen et al. 2003) contains a 20 mm diameter cylindrical diameter inclusion that is three times stiffer than the background (Madsen et al. 2003). The Young's modulus of the background material was 40 kPa, while the inclusion possessed a Young's modulus of 120 kPa measured using the ELF 3200 mechanical testing system (EnduraTEC, Minnetonka, MN, USA) in our laboratory.

The TM phantom immersed in a safflower oil bath was scanned using an Aloka SSD 2000 real-time clinical ultrasound scanner (Aloka Inc., Tokyo, Japan), using a 7.5 MHz linear array transducer with an approximate 70% bandwidth. The linear array transducer provided 220 A-lines in a single RF data frame. A single transmit focus was set at a depth of 55 mm in the phantom, with dynamic focusing on receive. A compression plate with a rectangular slot to match the transducer face was mounted a linear translation stage driven by a stepper motor controlled by a personal computer. The compression plate was larger than the phantom surface and provided a uniform compression of the phantom. Echo signals were acquired originating from the top of the phantom to a depth of 9 cm before and after an applied compression of 0.5% of the phantom height. An initial precompression of 3% was applied to ensure proper contract between the compression plate and the phantom. The oil provides a thin film of oil on the top and bottom surfaces of the phantom, to ensure slip boundary conditions.

Ultrasound RF signals were digitized using a 12-bit data acquisition board (Gage Applied Technologies Inc., Quebec, Canada) at a sampling rate of 100 MHz. The RF data were stored in a personal computer for off-line analysis. The pre- and postcompression RF echo signals were then analyzed using both the two-step and the traditional cross-correlation method using different windows lengths. The first correlation step for the two-step cross-correlation method used nonoverlapped gated windows with 20 wavelength window length. The second step of two-step cross-correlation method used the same window length as the traditional cross-correlation method shown in Fig. 3. As shown in Fig. 3a–f, the second step window lengths were 1, 2, 3, 6, 8 and 10 wavelengths, respectively. The overlap factor or shift between the two adjacent data segments for both the traditional and second step of the two-step method was fixed at two wavelengths.

RESULTS

Simulation

In this section, we present elastograms showing the performance of the two-step cross-correlation algorithm in improving the ability to resolve two inclusions with varying separations simulated using FEA. Local displacements and strains between the pre- and postcompression RF data are estimated by using both traditional cross-correlation and the two-step cross-correlation method. Axial strain is estimated using a five-point least-squares strain estimator from displacement data (Kallel and Ophir 1997). For displacements estimated using the single wavelength window, with a 75% overlap, this corresponds to a data length of 5 mm (2.5 wavelengths) over which each local strain estimate is obtained. Figure 2 presents the ideal strains images from ANSYS simulations, along with the estimated axial strain images using the two-step correlation method, and elastograms obtained using the traditional cross-correlation method for inclusion center separations of 1, 2, 3 and 4 mm, respectively. The two-step cross-correlation method utilized a 20 wavelength window length for the first step and a one wavelength window for the second step, with corresponding overlaps of 0% and 75% for

first and second steps, respectively. The window length for the traditional cross-correlation method utilized both one and 20 wavelength windows with a 75% overlap in the data segments, respectively.

Note that the elastograms obtained with the new two-step cross-correlation method provide a clearer delineation between the two stiffer inclusions in the simulated phantom. The two-step method provides a clear discrimination of inclusions that are 2 mm apart, as illustrated in Fig. 2. The two step method provides significantly lower noise levels when compared to the traditional cross-correlation method using the smaller one wavelength window and better axial resolution when compared with the traditional cross method with 20 wavelength window. Axial resolution in elastography was measured using the distance between the full-widths at half-maximum of the strain profiles of the two equally stiff lesions embedded in a softer homogeneous background.

Elastograms from experimental data

The strain estimation performance of the two-step cross-correlation algorithm was compared with the traditional cross-correlation method using pre- and post-compression data from a TM phantom, as described previously. Pairs of axial strain images obtained using the two-step and the traditional cross-correlation method for different window lengths are compared in Fig. 3. Note that the window length listed for the two-step method corresponds to the window length of the second correlation step in this figure. Comparison of the images illustrates that the two-step method is able to provide low-noise and high resolution images for window lengths that correspond to a single ultrasound wavelength. On the other hand, the traditional method requires a window length of around 10 wavelengths, as shown in Fig. 3f, to clearly discriminate the inclusion from the background.

As the window length increases from one wavelength to eight wavelengths, partial visualization of the inclusion and background are observed for the traditional cross-correlation method. The axial strain image of the top half of the background is visualized at a window length of around six wavelengths. The reason for the improvement of the noise properties of the strain image from the top to the bottom of the image is due to the increased displacement of the scatterers near the bottom of the phantom. To incorporate information regarding the displacement of these scatterers, larger window lengths are necessary. On the other hand, for the two-step method, since the first step utilizes a larger window length, the displacement information at deeper depths is obtained *a priori* to guide the second step of the procedure using a significantly smaller window length.

The results in Fig. 3 clearly demonstrate the utility of the two-step method. With a small increase in the processing time, the two-step method significantly improves the axial resolution of the displacement and strain estimates while maintaining the noise characteristics of the image. The next section presents quantitative results to demonstrate the improvement in the SNR_e and CNR_e obtained with the two-step method for the smaller window lengths.

Quantitative experimental results

Ultrasound RF data are obtained in a manner similar to that described in the previous section. A uniformly elastic phantom is utilized to obtain data to compute the mean and variance of the strain estimates and to calculate the corresponding SNR_e, while the single inclusion phantom is utilized to obtain CNR_e variations.

Bias and variance of strain estimation—Quantitative estimates of the mean and standard deviation of the strain estimates obtained using the two-step cross-correlation method are compared with the traditional cross-correlation method in Fig. 4. Strain estimates obtained

from a region-of-interest between a depth of 45 to 65 mm around the transmit focus of the transducer were utilized. An applied compression of 0.5% of the phantom height was used in this analysis. Note that the two-step method provides an accurate estimation of the applied strain, starting from a window length of one wavelength with no bias in the strain estimates. The smaller window lengths of less than a wavelength introduce a bias in the strain estimates, as seen in Fig. 4. The standard deviations of the strain estimates denoted by the error bars are also constant for all the window lengths used. On the other hand, a minimum window length of around eight wavelengths is necessary to obtain an unbiased strain estimate using the traditional cross-correlation method.

Figure 4 clearly illustrates that the two-step cross-correlation method provides more stable performance over a large range of window lengths. The standard deviation of the strain estimates with the two-step cross-correlation method is also significantly lower than that obtained with the traditional cross-correlation method for window lengths smaller than 10 wavelengths.

Signal-to-noise ratio comparison—The SNR_e in elastography is a quantity used to describe the noise properties of the strain image. The SNR_e is defined as (Cespedes 1993; Varghese and Ophir 1997),

$$SNR_e = \frac{m_s}{\sigma_s}, \tag{1}$$

where m_s and σ_s denote the mean and the standard deviation of estimated strain respectively.

Figure 5 shows the variation in the SNR_e obtained from the axial strain image of the uniformly elastic phantom using the two-step and traditional cross-correlation methods, respectively. When the window length is less than eight wavelengths, the two-step method provides a SNR_e level that is eight times that obtained using the traditional cross-correlation method. To obtain a comparable SNR_e with that obtained using the two-step method, the traditional cross-correlation method requires a window length greater than 10 wavelengths, where the two methods show a similar performance.

Contrast-to-noise ratio comparison—The CNR_e is a quantity that determines the detectability of lesions. The CNR_e for elastography is defined as follows (Varghese and Ophir 1998):

$$CNR_e = \frac{2(e_B - e_I)^2}{\sigma_{eB}^2 + \sigma_{eI}^2} \tag{2}$$

where e_B and e_I represent mean strain in the background and inclusion, while σ_{eB} and σ_{eI} represent standard deviation of background and inclusion, respectively.

The regions in the strain image corresponding to the inclusion and the background utilized in the computation of the CNR_e are shown in Fig. 6. Note that the region selected for the background differs from that utilized in previous papers (Varghese and Ophir 1998;Varghese et al. 2001). The regions were selected as shown in Fig. 6, since this scheme enables the repeatable selection of the same regions across strain images and the user only has to select the inclusion center. Observe, from Fig. 6, that this scheme utilizes the region that includes the stress concentration artifacts for the background and would, in general, provide a higher value of the contrast and the CNR_e. The strain estimates for the inclusion are selected from a 10 × 10 mm rectangular region at the inclusion center while the strain estimates for the background

are selected from two 10 × 4 mm rectangular regions located at the left and right sides of the inclusion, respectively.

As shown in Fig. 7, the CNR_e values obtained with the two-step cross- correlation method is larger than that obtained with the traditional cross-correlation method at all window lengths. However, for window lengths smaller than 10 wavelengths and to a single wavelength, the two-step method provides a significantly larger value of the CNR_e, while that obtained with traditional cross-correlation is close to zero.

DISCUSSION AND CONCLUSIONS

A two-step cross-correlation method is proposed to estimate the axial displacement and strain in a medium subjected to a unidirectional quasistatic compression. This method enables the use of window lengths on the order of a single wavelength to estimate tissue displacements and strain, while preserving the noise properties of the strain image. The traditional one-dimensional cross-correlation method requires a window length of at least 10 wavelengths to provide comparable noise characteristics in the strain image.

The two-step cross-correlation method proposed in this paper enables the use of processing windows on the order of a wavelength by estimating the local displacements in two steps. In the first step, a larger window length (>10 wavelengths) with no overlapping of the data segments in the cross-correlation processing is utilized to obtain a coarse but high-SNR estimate of the local displacement. The coarse displacement estimate is then interpolated to obtain a fine local displacement map that guides the second cross-correlation step using the single wavelength processing window. Displacements estimated using the first cross-correlation step are not utilized to form the final strain elastogram and are utilized only to guide the positioning or localization of the gated window in the corresponding postcompression echo signals. This enables placement of the postcompression window to lie near the location to which the tissue scatterers were displaced during the axial compression. This leads to the improved resolution obtained with the use of the single wavelength window in the second cross-correlation step.

Simulation and experimental results demonstrate the utility of the two-step cross-correlation method. Simulation results shown in this paper demonstrate that this method can discriminate between two 2 mm stiffer inclusions that are separated by 2 mm. Experimental results demonstrate the ability to obtain strain images using a single wavelength processing window, as opposed to the 10 wavelength window required for the traditional cross-correlation method.

The use of small processing windows with high overlap can significantly improve the axial resolution in the strain images for clinical diagnosis (Alam et al. 2000; Righetti et al. 2002). The algorithm proposed in this paper requires approximately twice the signal processing or computational load. However, this is not a significant limitation, since 1-D cross-correlation algorithms can function in real-time with frames rate on the order of 10–15 frames/s using the 10 wavelength window. Since the first step in the two-step method utilizes coarse displacement estimates, this step is significantly faster when compared with the second step; therefore, the drop-off in performance is not as significant, when compared with the traditional method obtained at the same window length. The increase in the computational time for the two-step cross-correlation method was about 8% higher when compared with the traditional cross-correlation processing with the smaller window length utilized in the two-step method. The processing time will further improve with technological developments in computer processing speed.

Acknowledgements

This work was supported in part by NIH grant R21 EB003853.

References

Alam SK, Ophir J. Reduction of signal decorrelation from mechanical compression of tissues by temporal stretching: Applications to elastography. Ultrasound Med Biol 1997;23:95–105. [PubMed: 9080622]

Alam SK, Ophir J, Konofagou EE. An adaptive strain estimator for elastography. IEEE Trans Ultrason Ferroelect Freq Cont 1998;45:461–472.

Alam SK, Ophir J, Varghese T. Elastographic axial resolution criteria: An experimental study. IEEE Trans Ultrason Ferroelect Freq Cont 2000;47:304–309.

Bilgen M, Insana MF. Deformation models and correlation analysis in elastography. J Acoust Soc Am 1996;99:3212–3224. [PubMed: 8642127]

Bilgen M, Insana MF. Error analysis in acoustic elastography. II. Strain estimation and SNR analysis. J Acoust Soc Am 1997;101:1147–1154. [PubMed: 9035402]

Brusseau E, Perrey C, Delachartre P, Vogt M, Vray D, Ermert H. Axial strain imaging using a local estimation of the scaling factor from RF ultrasound signals. Ultrason Imaging 2000;22:95–107. [PubMed: 11061461]

Cespedes, EI. Elastography: Imaging of biological tissue elasticity. University of Houston; 1993. Ph.D. Dissertation

Cespedes I, Ophir J, Ponnekanti H, Maklad N. Elastography: Elasticity imaging using ultrasound with application to muscle and breast *in vivo*. Ultrason Imaging 1993;15:73–88. [PubMed: 8346612]

Chaturvedi P, Insana MF, Hall TJ. 2-D compounding for noise reduction in strain imaging. IEEE Trans Ultrason Ferroelect Freq Cont 1998;45:179–191.

Chen EJ, Adler RS, Carson PL, Jenkins WK, O'Brien WD Jr. Ultrasound tissue displacement imaging with application to breast cancer. Ultrasound Med Biol 1995;21:1153–1162. [PubMed: 8849830]

Hall TJ, Zhu Y, Spalding CS. In vivo real-time freehand palpation imaging. Ultrasound Med Biol 2003;29:427–435. [PubMed: 12706194]

Kallel F, Ophir J. A least-squares strain estimator for elastography. Ultrason Imaging 1997;19:195–208. [PubMed: 9447668]

Li Y, Zagzebski JA. A frequency domain model for generating B-mode images with array transducers. IEEE Trans Ultrason Ferroelect Freq Cont 1999;46:690–699.

Madsen EL, Frank GR, Krouskop TA, Varghese T, Kallel F, Ophir J. Tissue-mimicking oil-in-gelatin emulsions for use in heterogeneous elastography phantoms. Ultraso Imaging 2003;25:17–38.

O'Donnell M, Skovoroda AR, Shapo BM, Emelianov SY. Internal displacement and strain imaging using ultrasonic speckle tracking. IEEE Trans Ultrason Ferroelect Freq Cont 1994;41:314–325.

Ophir J, Cespedes I, Ponnekanti H, Yazdi Y, Li X. Elastography: a quantitative method for imaging the elasticity of biological tissues. Ultrason Imaging 1991;13:111–134. [PubMed: 1858217]

Pellot-Barakat C, Frouin F, Insana MF, Herment A. Ultrasound elastography based on multiscale estimations of regularized displacement fields. IEEE Trans Med Imaging 2004;23:153–163. [PubMed: 14964561]

Righetti R, Ophir J, Ktonas P. Axial resolution in elastography. Ultrasound Med Biol 2002;28:101–113. [PubMed: 11879957]

Shi H, Varghese T. Two-dimensional multi-level strain estimation for discontinuous tissue. submitted

Srinivasan S, Kallel F, Souchon R, Ophir J. Analysis of an adaptive strain estimation technique in elastography. Ultrason Imaging 2002;24:109–118. [PubMed: 12199417]

Srinivasan S, Ophir J, Alam SK. Elastographic imaging using staggered strain estimates. Ultrason Imaging 2002;24:229–245. [PubMed: 12665239]

Srinivasan S, Righetti R, Ophir J. Trade-offs between the axial resolution and the signal-to-noise ratio in elastography. Ultrasound Med Biol 2003;29:847–866. [PubMed: 12837500]

Srinivasan S, Righetti R, Ophir J. An experimental characterization of elastographic spatial resolution: Analysis of the trade-offs between spatial resolution and contrast-to-noise ratio. Ultrasound Med Biol 2004;30:1269–1280. [PubMed: 15582226]

Talhami HE, Wilson LS, Neale ML. Spectral tissue strain: A new technique for imaging tissue strain using intravascular ultrasound. Ultrasound Med Biol 1994;20:759–772. [PubMed: 7863565]

Varghese T, Bilgen M, Ophir J. Multiresolution imaging in elastography. IEEE Trans Ultrason Ferroelect Freq Cont 1998;45:65–75.

Varghese T, Ophir J. Performance optimization in elastography: Multicompression with temporal stretching. Ultrason Imaging 1996;18:193–214. [PubMed: 9123673]

Varghese T, Ophir J. A theoretical framework for performance characterization of elastography: The strain filter. IEEE Trans Ultrason Ferroelect Freq Cont 1997;44:164–172.

Varghese T, Ophir J. An analysis of elastographic contrast-to-noise ratio. Ultrasound Med Biol 1998;24:915–924. [PubMed: 9740393]

Varghese T, Ophir J. Characterization of elastographic noise using the envelope of echo signals. Ultrasound Med Biol 1998;24:543–555. [PubMed: 9651964]

Varghese T, Ophir J, Konofagou E, Kallel F, Righetti R. Tradeoffs in elastographic imaging. Ultrason Imaging 2001;23:216–248. [PubMed: 12051276]

Wagner RF, Smith SW, Sandrik JM, Lopez H. Statistics of speckle in ultrasound B-scans 1983;SU-30:156–163.

Yamakawa M, Shiina T. Strain estimation using the extended combined autocorrelation method. Jpn J Applied Physics Part 1 2001;40:3872–3876.

Zhu Y, Hall TJ. A modified block matching method for real-time freehand strain imaging. Ultrason Imaging 2002;24:161–176. [PubMed: 12503771]

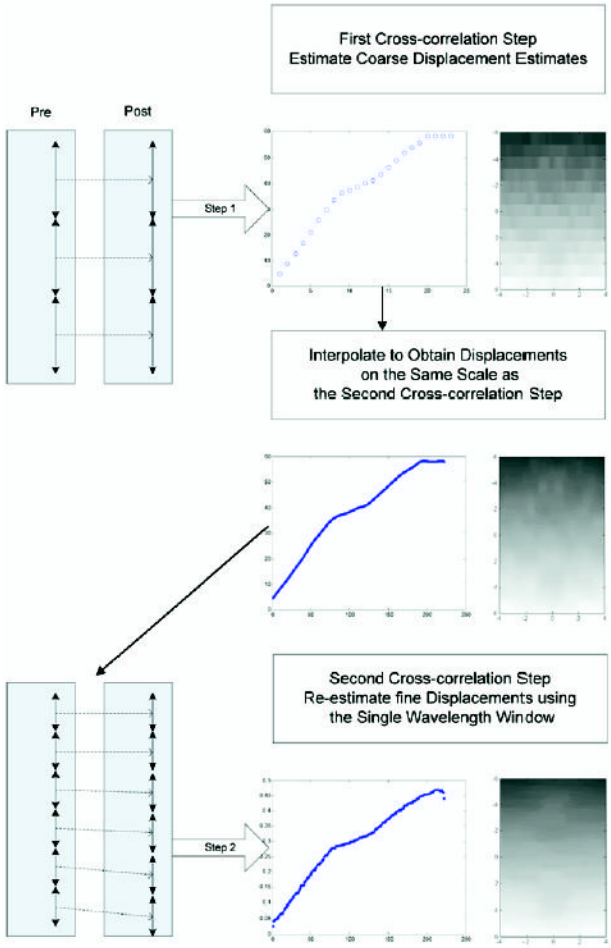

Fig. 1.

Flow chart describing the two correlation steps in the two-step cross-correlation method. The two cross-correlation steps are clearly illustrated in the figure. The interpolation step is utilized only to guide the placement of the window in the postcompression echo signals for the second cross-correlation step.

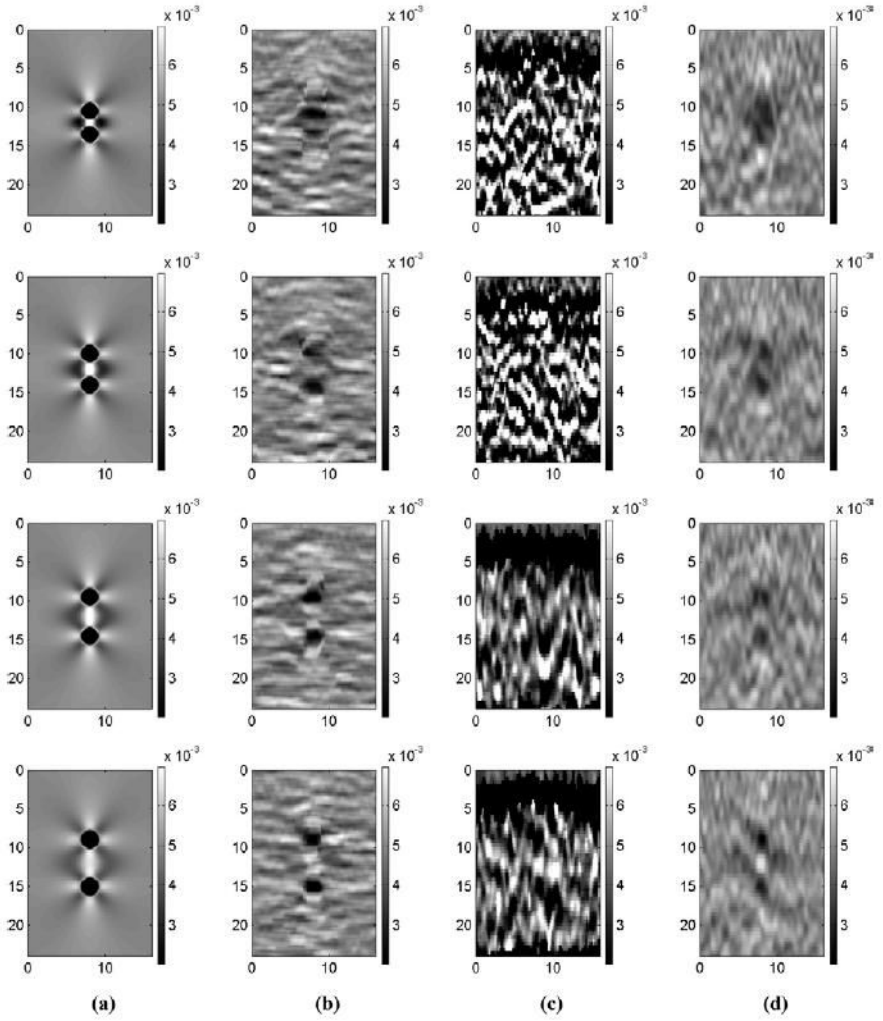

Fig. 2.

Axial strain images from a simulated ANSYS phantom with two stiffer inclusions separated by 1 mm (i), 2 mm (ii), 3 mm (iii) and 4 mm (iv), respectively. The ideal strain image is shown in (a), while the image obtained using the two step method is shown in (b). The strain images obtained using window length of one and 20 wavelengths corresponding to the second and first step of the two step method are shown in (c) and (d), respectively. The height and width of the axial strain image are in dimensions of millimeters.

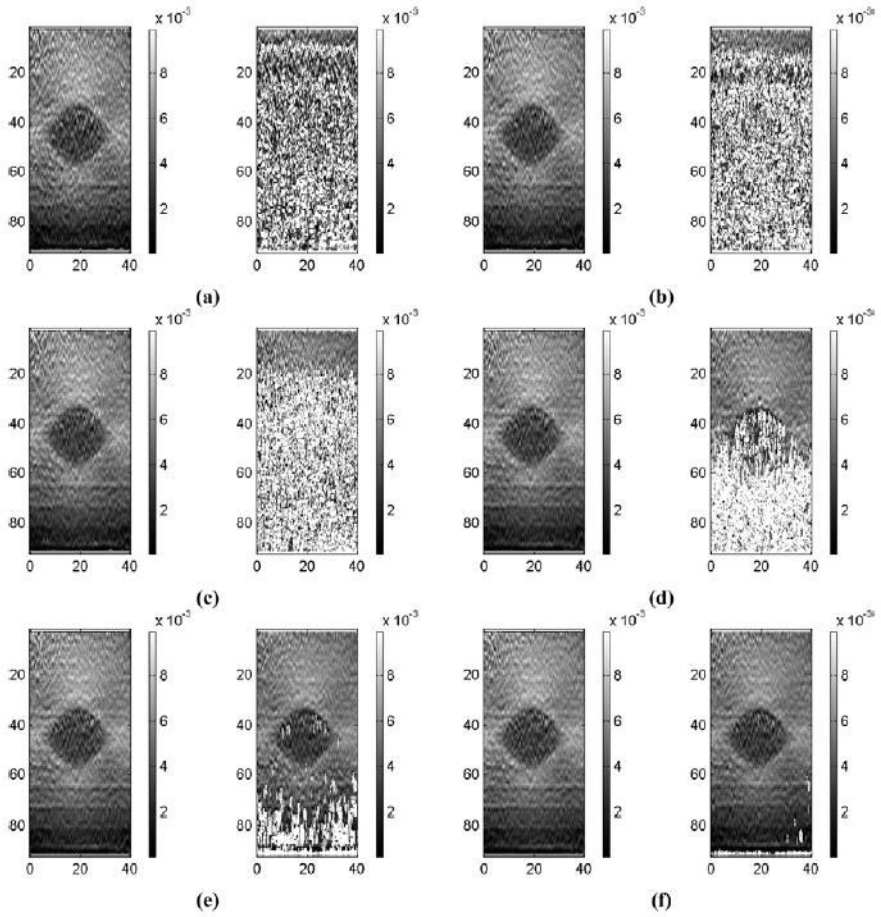

Fig. 3.

Comparison of the axial strain images of a TM inclusion phantom obtained using the two-step cross-correlation method and the traditional cross-correlation method using different window lengths of (a) one wavelength; (b) two wavelengths; (c) three wavelengths; (d) six wavelengths; (e) eight wavelengths; (f) 10 wavelengths. For the two-step method, the window length denotes the size of the window in the second correlation step with a 20 wavelength window utilized for the first step. The height and width of the axial strain image are in dimensions of millimeters.

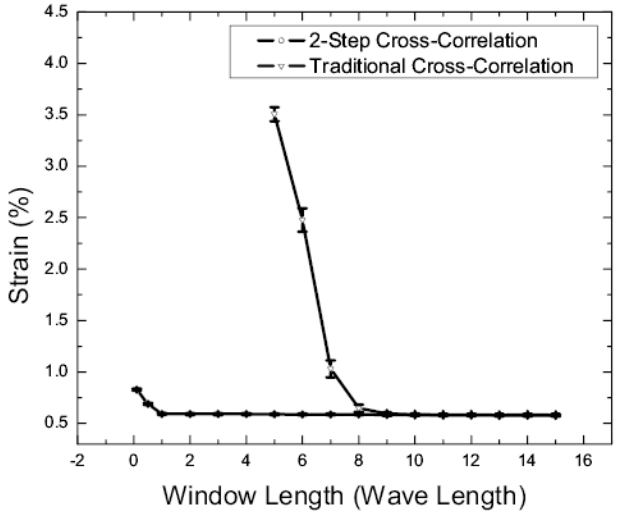

Fig. 4.

Plots of the mean strain estimate along with the error-bars over 10 independent realizations *vs.* the window length starting from 0.1 wavelengths to 12 wavelengths (for a 7.5 MHz center frequency, a window length of one wavelengths equals 0.2 mm). The error bars denote the standard deviation of the strain estimates.

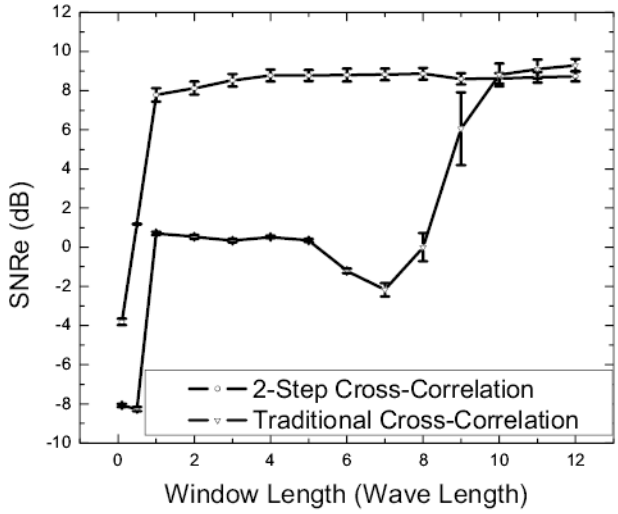

Fig. 5.

Plots of SNR_e *vs.* the window length for the two-step cross-correlation and the traditional method. Note the improvement in SNR_e the with a window length of a single wavelength in the second correlation step of the two-step method. A similar improvement in the SNR_e is obtained using a 10 wavelength window for the traditional cross-correlation method.

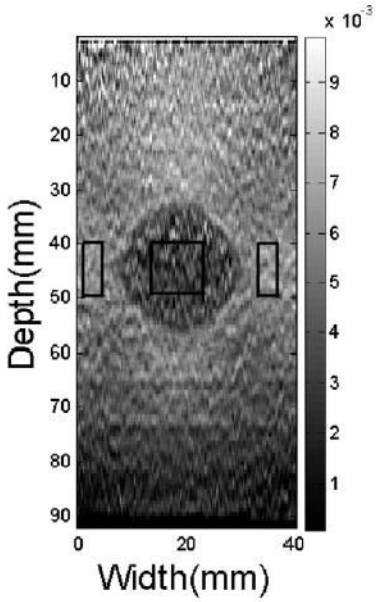

Fig. 6.

Diagram illustrating the regions utilized in the strain image to compute the CNR_e. Note that we utilize the region that includes the stress concentration artifacts, which provides the highest contrast but differs in the traditional estimation of the CNR_e.

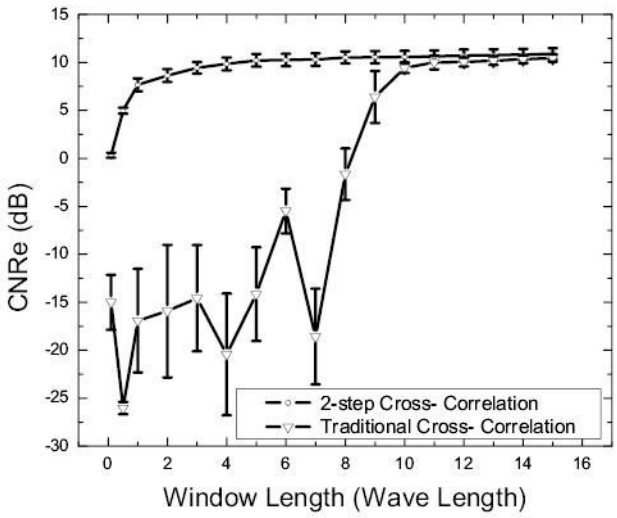

Fig. 7.
Plots of CNR_e *vs.* the window length for the two-step cross-correlation and the traditional methods.